*Int. J. Solids Structures*, 1969, Vol. 5, pp. 1095 to 1105. Pergamon Press. Printed in Great Britain

# CLOSED-FORM SOLUTIONS TO PROBLEMS OF WAVE PROPAGATION IN A RIGID, WORKHARDENING, LOCKING ROD*

R. C. SHIEH, G. A. HEGEMIER and W. PRAGER

Department of the Aerospace and Mechanical Engineering Sciences
University of California, San Diego
La Jolla, California

**Abstract**—One-dimensional wave propagation in a semi-infinite, rigid, workhardening, locking rod is considered. The general problem is discussed and closed-form solutions are obtained for several special cases. It is anticipated that the latter will provide useful check-cases for numerical programs designed to cope with wave propagation in media with complex constitutive laws. The stipulated mechanical behavior is also interesting in its own right since it is qualitatively typical of soils in uniaxial compressive strain.

## 1. INTRODUCTION

SINCE the second world war, plastic wave propagation has been a particularly active field of applied mechanics. Whereas Hooke's law is generally accepted as an adequate foundation for the theoretical study of elastic waves, a wide variety of constitutive laws are used in the theoretical investigation of plastic waves, and the experimental verification of theoretical predictions becomes essential. When the complexities of shape, loading process and material behavior are taken into account, this verification is rendered difficult by the following facts:

(i) numerical procedures based on *discrete* models must be used to obtain the "theoretical results" that are to be compared with the experimental evidence, and
(ii) for the nonlinear problems of plastic wave propagation, the manner in which this discretization may distort the solution is less well understood than for the linear problems of elastic wave propagation.

The fact that, for a specific problem, the numerical solution based on a discrete model agrees well with the results of an experiment does not, by itself, prove that the model is satisfactory. Indeed, for the specific problem on hand, the effects of the discretization may tend to compensate for a possible inadequacy in the constitutive equation.

It therefore becomes desirable that the numerical results furnished by discrete models be compared with exact, closed-form solutions, wherever solutions of this kind can be obtained by appropriate idealizations of shape, loading process, and constitutive equation. In the present paper, an exact, closed-form solution is developed for the propagation of longitudinal waves in a semi-infinite rod of rigid, workhardening, locking material. The rod is subjected to a compressive end-stress, which *first increases monotonically from zero to a maximum value and then decreases monotonically from this value to zero.* The assumed

* The results presented in this paper were obtained in the course of research sponsored by the Defense Atomic Support Agency under Contract DASA 01-68-C-0017.

mechanical behavior of the rod material is shown by the solid lines in Fig. 1. Consider first the behavior under monotonically *increasing* uniaxial Lagrangian compressive stress $\sigma$: until this stress reaches the yield limit $\sigma_y$, the material remains rigid (segment $OA$); thereafter, the increments of compressive† stress and strain, $d\sigma$ and $d\varepsilon$, are related by $d\sigma = K\, d\varepsilon$, where the constant $K$ is the workhardening modulus (segment $AD$); the material *locks* when the strain attains the value $\varepsilon^*$, that is, regardless of how much the stress is increased above the corresponding value $\sigma^*$, no further increase in strain occurs (segment $DE$). Finally, whenever the stress is decreased, the strain remains constant (segments $BC$ and $DF$). The stipulated mechanical behavior is a reasonable idealization of the typical behavior of soils in uniaxial compressive strain. This behavior is schematically indicated by the dashed curve in Fig. 1. Kaliski, Nowacki and Wlodarczyk [1] have studied longitudinal wave propagation in a rod made of a material that is obtained from the material considered here when $\sigma_y$ is taken as zero.

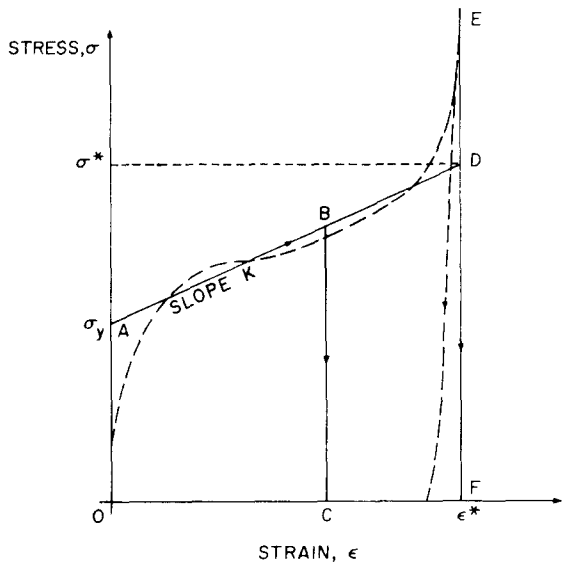


FIG. 1. Stress-strain diagram.

A general discussion of the problem on hand is given in Section 2. The special case of linearly increasing and decreasing end-stress is treated in Section 3.

## 2. GENERAL DISCUSSION OF PROBLEM

Let $t$ and $x$ be the time and the Lagrangian coordinate along the rod, and denote the compressive stress applied at the time $t$ to the end $x = 0$ by $p(t)$, the (infinitesimal) longitudinal displacement by $u(x, t)$, and the velocity by $v(x, t)$. With these notations, the equation of motion is

$$\partial\sigma/\partial x + \rho\, \partial v/\partial t = 0, \tag{1}$$

† Contrary to the usual sign convention, compressive stresses are regarded as positive in this paper.

where $\rho$ is the initial density of the homogeneous rod. Since $\varepsilon = -\partial u/\partial x$ and $v = \partial u/\partial t$, we have

$$\partial\varepsilon/\partial t + \partial v/\partial x = 0. \tag{2}$$

Equations (1) and (2), together with the appropriate boundary and initial conditions, and the stress–strain relations, determine the values of $\sigma$, $\varepsilon$, $v$ throughout the $x$–$t$ plane except at certain lines of discontinuity, which are classified as shock waves or weak discontinuities according to whether these variables themselves or their derivatives are discontinuous. If the symbols $\Delta\sigma$, $\Delta\varepsilon$, $\Delta v$ are used to indicate the discontinuous changes that occur as a shock wave sweeps across a particle, and if the equation of the shock wave in the $x$–$t$ plane is $x = \varphi(t)$, the following shock relations apply:

$$\Delta\sigma = \rho\varphi'(t)\,\Delta v = \rho[\varphi'(t)]^2\,\Delta\varepsilon. \tag{3}$$

Here $\varphi'(t) = \mathrm{d}\varphi/\mathrm{d}t$ is the velocity of propagation of the shock with respect to the undeformed configuration of the rod. At a weak discontinuity, $\sigma$, $\varepsilon$, and $v$ are continuous, and their values are obtained from the expressions valid in the region bounded by the weak discontinuity.

Referring to Fig. 2, we divide the $x$–$t$ plane into regions in which different analytical expressions are obtained for $\sigma$, $\varepsilon$ and $v$. The symbols $\sigma_n$, $\varepsilon_n$ and $v_n$ will be used to indicate stress, strain, and velocity in the $n$th region. The solution in each region is given by the following expressions:

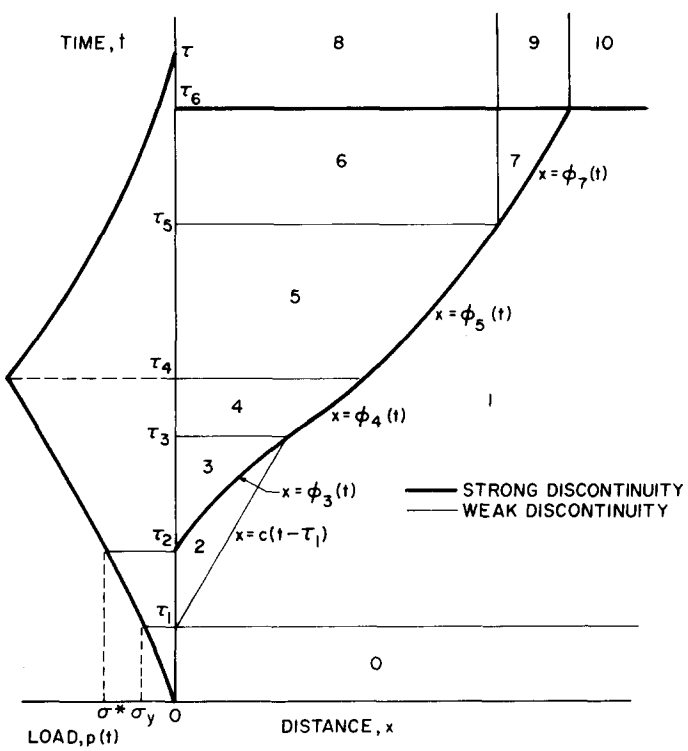


FIG. 2. Shock trajectory in the $x$–$t$ plane.

*Region* 0. The rod is at rest, and

$$\sigma_0 = p(t) \leq \sigma_y, \qquad \varepsilon_0 = v_0 = 0. \tag{4}$$

These expressions are valid for any $x \geq 0$ and for $0 \leq t \leq \tau_1$, where $\tau_1$ is the time at which the end-stress $p$ reaches the yield limit.

*Region* 1. This is a region of constant state, in which

$$\sigma_1 = \sigma_y, \qquad v_1 = \varepsilon_1 = 0. \tag{5}$$

*Region* 2. This region is separated from region 1 by the weak discontinuity line $x = c(t-\tau_1)$, where $c = \sqrt{(K/\rho)}$. In view of the continuity of $\sigma$, $\varepsilon$, $v$ across this line, the condition $\sigma_2(0, t) = p(t)$ at the end of the rod, and the stress–strain relation

$$\sigma_2 = \sigma_y + K\varepsilon_2, \tag{6}$$

the solution of (1) and (2) takes the form

$$\begin{aligned} \sigma_2(x, t) &= p(t-x/c), \\ v_2(x, t) &= [p(t-x/c)-\sigma_y]/(\rho c) = c\varepsilon_2(x, t). \end{aligned} \tag{7}$$

*Region* 3. This region is separated from region 2 by a *locking shock*. This starts at the point $t = \tau_2$ on the $t$-axis, where the end-stress reaches the value $\sigma^*$. The material in region 3 is in the locked state. Since this implies

$$\varepsilon_3 = \varepsilon^* = \text{const}, \tag{8}$$

the motion in region 3 is a rigid-body translation, that is, $v_3$ does not depend on $x$. If superimposed bars are used to indicate values at the shock, we have

$$v_3(t) = \bar{v}_3(t), \tag{9}$$

and (1) may be integrated with respect to $x$ to furnish

$$\sigma_3(x, t) - p(t) + \rho x v_3'(t) = 0, \tag{10}$$

where the prime denotes differentiation of a function with respect to its argument. At the shock $x = \phi_3(t)$, equation (10) becomes

$$\bar{\sigma}_3(t) - p(t) + \rho\varphi_3(t)\bar{v}_3'(t) = 0, \tag{11}$$

and the shock relations furnish

$$\bar{\sigma}_3 - \bar{\sigma}_2 = \rho\varphi_3'(\bar{v}_3 - \bar{v}_2) = \rho\varphi_3'^2(\varepsilon^* - \bar{\varepsilon}_2). \tag{12}$$

The second equality in (12) gives

$$\bar{v}_3 = \bar{v}_2 + \varphi_3'(\varepsilon^* - \bar{\varepsilon}_2). \tag{13}$$

Use of (13) in (11) and substitution of the result into the equation formed by the first and last members in (12) yields the following differential equation for $\varphi_3(t)$:

$$\begin{aligned} &p(t-\varphi_3/c) - p(t) + \frac{\varphi_3}{c}(1-\varphi_3'/c)^2 p'(t-\varphi_3/c) \\ &\quad + \tfrac{1}{2}\rho\{\varepsilon^* - [p(t-\varphi_3/c)-\sigma_y]/(\rho c^2)\}(\varphi_3^2)'' = 0. \end{aligned} \tag{14}$$

Note that the prime in (14) denotes differentiation of a function with respect to its argument, and that $\varphi_3(t)$ and $p(t-\varphi_3/c)$ have different arguments. Equation (14) must be integrated under the initial conditions

$$\varphi_3(\tau_2) = 0, \qquad \varphi_3'(\tau_2) = c. \tag{15}$$

Once $\varphi_3(t)$ is known, $v_3(t)$ can be obtained from (13) and (9), whereupon (10) provides $\sigma_3(x, t)$.

Since (14) is a nonlinear differential equation, a solution for an arbitrary loading function $p(t)$ is not readily obtainable. In general recourse must be made to numerical integration. In several special cases, however, region 3 vanishes and numerical procedures can be avoided. These cases are discussed under "Special Cases" at the end of this section.

*Region* 4. This region differs from the previous in that the state ahead of the shock is that of region 1, i.e. equation (5). Region 4 begins at $t = \tau_3$ which defines the point of intersection of the shock with the weak discontinuity line $x = c(t-\tau_1)$ emanating from $t = \tau_1$ on the $t$-axis. Following the discussion of region 3, we find:

$$\varepsilon_4 = \varepsilon^*, \tag{16}$$

$$v_4(t) = \bar{v}_4(t) = \varphi_4'(t)\varepsilon^*, \tag{17}$$

$$\bar{\sigma}_4(t) = \rho(\varphi_3')^2\varepsilon^* + \sigma_y, \tag{18}$$

$$\sigma_4(x, t) = p(t) - \rho\varepsilon^* x\varphi_4''(t), \tag{19}$$

where $\varphi_4(t)$ satisfies

$$(\varphi_4^2)'' = (2/\rho\varepsilon^*)[p(t)-\sigma_y], \tag{20a}$$

$$\varphi_4(\tau_3) = \varphi_3(\tau_3), \qquad \varphi_4'(\tau_3) = \varphi_3'(\tau_3). \tag{20b}$$

Upon integrating (20) and defining the following new variables:

$$F_{i+1}(t) = \int_{\tau_i}^{t}\int_{\tau_i}^{\xi} [p(\eta)-\sigma_y]\,\mathrm{d}\eta\,\mathrm{d}\xi, \tag{21}$$

$$G_{i+1}(t) = F_{i+1}'(t) = \int_{\tau_i}^{t} [p(\eta)-\sigma_y]\,\mathrm{d}\eta, \tag{22}$$

$$a = \varphi_3(\tau_3)\varphi_3'(\tau_3) = \text{const.} \tag{23}$$

the functions $\varphi_4$, $v_4$, and $\sigma_4$, become

$$\varphi_4(t) = [(2/\rho\varepsilon^*)F_4(t) + 2a(t-\tau_3) + \varphi_3^2(\tau_3)]^{1/2}, \tag{24}$$

$$v_4(t) = [G_4(t) + \rho a\varepsilon^*]/\rho\varphi_4(t), \tag{25}$$

$$\sigma_4(x, t) = p(t) + [x/\varphi_4(t)]\,[(\rho/\varepsilon^*)v_4^2(t) - (p(t)-\sigma_y)]. \tag{26}$$

*Region* 5. Unloading first takes place in this region. Referring to Fig. 2, it can be shown that $\bar{\sigma}$ (just behind the shock) increases from the value $\sigma^*$ at $t = \tau_2$ on the $t$-axis to a maximum at $x = \varphi_4(\tau_4)$, $t = \tau_4$ where $p(\tau_4) = \max p(t)$. For $t > \tau_4$, $\bar{\sigma}$ decreases with increasing $t$. The time $\tau_5$ is defined by $\bar{\sigma}(\tau_5) = \sigma^*$. Thus, in region 5 each point of the rod experiences the strain $\varepsilon = \varepsilon^*$; unloading therefore takes place along the segment $EF$ of the stress–strain diagram (Fig. 1). In view of this we conclude that the governing equations for $\sigma_5, \varepsilon_5, v_5, \varphi_5$

are of the same form as for region 4. Two cases, however, should be distinguished: 1) $\tau \geq \tau_5$ and 2) $\tau \leq \tau_5$. Here $\tau$ is defined by $p(\tau) = 0$. In the first case, ($\tau \geq \tau_5$), the solution in $\tau_4 \leq t \leq \tau_5$, which we denote by the subscript "5" is obtained from (24) to (26) by increasing the index $i$ by one and replacing $a$ by $[G_4(\tau_4)+\rho\varepsilon^* a]/\rho\varepsilon^*$ (the latter accounts for the proper initial condition at $t = \tau_4$); this gives

$$\varphi_5(t) = \{(2/\rho\varepsilon^*)F_5(t)+(2/\rho\varepsilon^*)[G_4(\tau_4)+\rho\varepsilon^* a](t-\tau_4)+\varphi_4^2(\tau_4)\}^{1/2}, \tag{27}$$

$$v_5(t) = [G_5(t)+G_4(\tau_4)+\rho\varepsilon^* a]/\rho\varphi_5(t), \tag{28}$$

$$\sigma_5(x,t) = p(t)+[x/\varphi_5(t)][(\rho/(\varepsilon^*)v_5^2(t))-(p(t)-\sigma_y)], \tag{29}$$

$$\varepsilon_5 = \varepsilon^*, \tag{30}$$

where we have employed the relation (c.f. (24))

$$\rho\varepsilon^*\varphi_4(\tau_4)\varphi_4'(\tau_4) = G_4(\tau_4)+\rho\varepsilon^* a. \tag{31}$$

In the second case ($\tau \leq \tau_5$) the solution in $\tau_4 \leq t \leq \tau$ is again given by (27)–(30). The solution in $\tau \leq t \leq \tau_5$, however, which we denote by the subscript "5'", is obtained by setting $p(t) = 0$ and solving (20a) subject to the initial conditions $\varphi_{5'}(\tau) = \varphi_5(\tau)$, $\varphi_{5'}'(\tau) = \varphi_5'(\tau)$; the result is

$$\varphi_{5'}(t) = \{\varphi_5^2(\tau)+2\varphi_5(\tau)\varphi_{5'}(\tau)(t-\tau)-\sigma_y(t-\tau)^2(\rho\varepsilon^*)^{-1}\}^{1/2} \tag{32a}$$

or, in terms of $G_i$,

$$\varphi_{5'}(t) = (\rho\varepsilon^*)^{-1/2}\{-\sigma_y(t-\tau)^2+2[G_5(\tau)+G_4(\tau_4)+\rho\varepsilon^* a](t-\tau) + \rho\varepsilon^*\varphi_5^2(\tau)\}^{1/2}. \tag{32b}$$

In addition we have

$$v_{5'}(t) = [\rho\varphi_{5'}(t)]^{-1}[-\sigma_y(t-\tau)+G_5(\tau)+G_4(\tau_4)+\rho\varepsilon^* a], \tag{33}$$

$$\sigma_{5'}(x,t) = [x/\varphi_{5'}(t)][\sigma_y+(\rho/\varepsilon^*)v_{5'}^2(t)], \tag{34}$$

$$\varepsilon_5' = \varepsilon^*. \tag{35}$$

Finally, we note that an implicit relation for $\tau_5$ can be obtained by setting $t = \tau_5$ and $\bar{\sigma}_5(\tau_5) = \sigma^*$ in (29), which yields

$$\left(\frac{\sigma^*-\sigma_y}{\rho\varepsilon^*}\right)^{1/2} = c = \frac{G_5(\tau_5)+G_4(\tau_4)+\rho\varepsilon^* a}{\rho\varepsilon^*\varphi_5(\tau_5)} = \varphi_{5'}(\tau_5) = \frac{v_5(\tau_5)}{\varepsilon^*}. \tag{36}$$

*Regions 6 and 7.* When $\bar{\sigma}_5$ attains the value $\sigma^*$ (at $\tau = \tau_5$), which marks the end of region 5, the state of stress and strain just behind the shock corresponds to point $D$ of Fig. 1. With further unloading a new region, region 7, develops in which each point of the rod unloads along a segment such as $BC$ in Fig. 1. The adjacent region, which we designate as region 6, differs from the previous in that each point unloads only along the segment DF.

Employing the shock relations (3) we have

$$\bar{\sigma}_7-\sigma_y = \rho\varphi_7'\bar{v}_7 = \rho(\varphi_7')^2\bar{\varepsilon}_7. \tag{37a}$$

Noting that $(\bar{\sigma}_7-\sigma_y)/\bar{\varepsilon}_7 = K$, equation (35) implies

$$\varphi_7'(t) = c, \tag{37b}$$

whereupon

$$\varphi_7(t) = c(t-\tau_5)+\varphi_5(\tau_5). \tag{37c}$$

Since $\varepsilon = \varepsilon(x)$ in regions 6 and 7, equation (2) indicates that

$$v_6(t) = v_7(t) = \bar{v}_7(t). \tag{38}$$

By virtue of (38), equation (1) may be integrated with respect to $x$ to give

$$\sigma_6(x, t) = \sigma_7(x, t) = p(t)-\rho x\dot{\bar{v}}_7(t). \tag{39}$$

Evaluating (39) at the shock and using the first equality of (37a) to eliminate $\bar{\sigma}_7$, we ascertain that $\bar{v}_7$ satisfies the following differential equation:

$$\rho[c(t-\tau_5)+\varphi_5(\tau_5)]\frac{d\bar{v}_7}{dt}+\rho c\bar{v}_7 = p(t)-\sigma_y. \tag{40a}$$

The appropriate initial condition is

$$\bar{v}_7(\tau_5) = \bar{v}_5(\tau_5). \tag{40b}$$

With the aid of (36), the solution of (40) can be written

$$\bar{v}_7(t) = [G_5(t)+G_4(\tau_4)+\rho\varepsilon^* a]/\{\rho[c(t-\tau_5)+\varphi_5(\tau_5)]\}. \tag{41}$$

Upon substituting (41) into (39), the following expression for the stresses is obtained:

$$\sigma_6(x, t) = \sigma_7(x, t) = p(t)-x[p(t)-\sigma_y-c\rho v_7(t)]/\varphi_7(t). \tag{42}$$

Finally, the strains are given by

$$\varepsilon_6 = \varepsilon^*, \tag{43a}$$

$$\varepsilon_7(x) = \bar{\varepsilon}_7(x) = (\bar{\sigma}_7-\sigma_7)/(\rho c^2) = (\rho cx)^{-1}[G_5(f(x))+G_4(\tau_4)+\rho\varepsilon^* a] \tag{43b}$$

where

$$f(x) = \varphi_7^{-1}(x) = \tau_5+(x-\varphi_5(\tau_5))/(c). \tag{43c}$$

The foregoing solutions are valid for $\tau_5 \le t < \tau_6$, where $\tau_6$ is defined by $\bar{\sigma}_7(\tau_6) = \sigma_y$. We note that if $\tau_6 > \tau$ the solution in $\tau \le t < \tau_6$ can be obtained from equation (41) to (43) by setting $p(t) = 0$ and replacing $G_5(t)$ by $G_5(\tau_5)-\sigma_y(t-\tau)$.

*Regions* 8–10. The point $x = \varphi_7(\tau_6^-)$, $t = \tau_6^-$ on the shock trajectory corresponds to the point $A$ in Fig. 1. Any further unloading results in an unloading wave with infinite velocity (since the slope of the segment $AO$ in Fig. 1 is infinite). In the $x$–$t$ plane this unloading wave leads to a discontinuity along $t = \tau_6$. For $t > \tau_6$ (regions 8, 9 and 10 of Fig. 2) the resulting states are

$$v_8 = v_9 = v_{10} = 0, \tag{44}$$

$$\sigma_8(t) = \sigma_9(t) = \sigma_{10}(t) = p(t), \tag{45}$$

$$\varepsilon_8 = \varepsilon^*, \qquad \varepsilon_9(x) = \varepsilon_7(x), \qquad \varepsilon_{10} = 0. \tag{46}$$

At $\tau = \tau_6^-$ equation (36) indicate $\bar{v}_7(\tau_6^-) = \bar{\varepsilon}_7(\tau_6^-) = 0$. Equation (41) in turn furnishes the following implicit relation for $\tau_6$:

$$G_5(\tau_6) + G_4(\tau_4) + \rho\varepsilon^* a = 0. \tag{47}$$

Substituting (47) into (42) we find

$$\sigma_7(\tau_6^-) = \sigma_6(\tau_6^-) = p(\tau_6) - x\frac{[p(\tau_6) - \sigma_y]}{c(\tau_6 - \tau_5) + \varphi_5(\tau_5)}. \tag{48}$$

Further, from (5) we have

$$\sigma_1(\tau_6^-) = \sigma_y. \tag{49}$$

Comparing (48) and (49) with (45) we see that the line $t = \tau_6$ is a strong discontinuity.

In deriving (44)–(49) we have used the fact that $\sigma_6(x, t)$ decreases monotonically with $x$ from the value $\sigma_y$ at the shock to the value $p(\tau_6) < \sigma_y$ at $x = 0$. The latter is demonstrated by (47), i.e. for (47) to be satisfied at $t = \tau_6^-$ it is necessary that $p(\tau_6^-) < \sigma_y$ (see the definition of $G_i$ in (22)).

*Special cases*

We conclude Section 2 by noting the following cases which lead to simplification of the foregoing results:

(i) If the segment AD of Fig. 1 has zero slope, then regions 2, 3 and 6, 7 vanish (i.e. $\tau_2, \tau_3 \to \tau_1$ and $\tau_3 \to \tau_2$ respectively) and regions 8, 9 coalesce. The solution forms for this case can be obtained from the general relations in the limit as $c \to 0$.

(ii) If $\sigma_y = 0$, then $\tau_6 = \infty$ and thus regions 6, 7 extend to infinity.

(iii) If $p(t)$ is suddenly applied such that $p(0^+) \geq \sigma^*$, then $\tau_3 = \tau_2 = \tau_1 = 0$ and regions 2, 3 vanish.

## 3. EXAMPLES

We now illustrate the foregoing theory with a few examples.

*Example* 1.

Let $p(t)$ be defined as follows:

$$\begin{aligned} p(t) &= 0 && \text{for } t < 0 \\ &= P_0 + (P_m - P_0)(t/\tau_4) && \text{for } 0 < t \leq \tau_4 \\ &= P_m[1 - (t - \tau_4)/(\tau - \tau_4)] && \text{for } \tau_4 \leq t \leq \tau \\ &= 0 && \text{for } t \geq \tau \end{aligned} \tag{50}$$

where $P_m \geq P_0 \geq \sigma^*$. This is the case (iii) mentioned in the last of section 2, and regions 2 and 3 of Fig. 2 vanish ($\tau_3 = \tau_2 = \tau_1 = 0$).

In view of (50), the functions $F_i$, $G_i$, $a$, as defined by (21) to (23), become

$$\begin{aligned} F_4(t) &= \tfrac{1}{2}(\alpha + \beta t/3)t^2, \\ G_4(t) &= (\alpha + \beta t/2)t \\ F_5(t) &= \tfrac{1}{2}\{\gamma(t - \tau_4)^2 - \lambda[(t^3 - \tau_4^3)/3 - \tau_4^2(t - \tau_4)]\}, \\ G_5(t) &= \gamma(t - \tau_4) - (\lambda/2)(t^2 - \tau_4^2), \\ a &= 0, \end{aligned} \tag{51a}$$

where

$$\begin{aligned}\alpha &= P_0-\sigma_y,\\ \beta &= (P_m-P_0)/\tau_4,\\ \gamma &= P_m[1+\tau_4/(\tau-\tau_4)]-\sigma_y,\\ \lambda &= P_m/(\tau-\tau_4).\end{aligned} \tag{51b}$$

Referring to Fig. 2, the solution is obtained as follows:
*Region* 1.

$$\sigma_1 = \sigma_y, \qquad \varepsilon_1 = v_1 = 0 \tag{52}$$

*Region* 4. Noting that (20b) reduces to $\varphi_4(0) = 0$, $\varphi_4'(0) = [(P_0-\sigma_y)/(\rho\varepsilon^*)]^{1/2}$, the solutions (24) to (26) become

$$\begin{aligned}\varphi_4(t) &= (t)[(\alpha+\beta t/3)/(\rho\varepsilon^*)]^{1/2},\\ v_4(t) &= (\alpha+\beta t/2)(\varepsilon^*/\rho)^{1/2}/(\alpha+\beta t/3)^{1/2},\\ \sigma_4(x,t) &= \alpha+\sigma_y+\beta t-\beta x[(\alpha+\beta t/4)(\rho\varepsilon^*)^{1/2}/3(\alpha+\beta t/3)^{3/2}],\\ \varepsilon_4 &= \varepsilon^*.\end{aligned} \tag{53}$$

*Region* 5. Using (53) to evaluate $\varphi_4(\tau_4)$ we find, from equations (27) to (30),

$$\begin{aligned}\varphi_5(t) &= (\rho\varepsilon^*)^{-1/2}\{\gamma(t-\tau_4)^2-\lambda[(t^3-\tau_4^3)/(3)-\tau_4^2(t-\tau_4)]\\ &\quad +2\tau_4(\alpha+\beta\tau_4/2)(t-\tau_4)+\tau_4^2(\alpha+\beta\tau_4/3)\}^{1/2},\\ v_5(t) &= [\gamma(t-\tau_4)-\lambda(t^2-\tau_4^2)/(2)+\tau_4(\alpha+\beta\tau_4/2)]/\rho\varphi_5(t),\\ \sigma_5(x,t) &= \gamma+\sigma_y-\lambda t-[x/\varphi_5(t)][(\gamma-\lambda t)-(\rho/\varepsilon^*)v_5^2(t)],\\ \varepsilon_5 &= \varepsilon^*.\end{aligned} \tag{54}$$

Equations (54) remain valid in the interval $\tau_4 \le t \le \tau_5 \le \tau$. If $\tau_5 > \tau$, then (32)–(35) must be employed for the interval $\tau \le t \le \tau_5$. For simplicity it will be assumed that $\tau_5 < \tau$. We note that the time $\tau_5$ is, by virtue of (36), defined implicitly by

$$\rho\varepsilon^* c\varphi_5(\tau_5) = \gamma(\tau_5-\tau_4)-\lambda(\tau_5^2-\tau_4^2)/2+\tau_4(\alpha+\beta\tau_4/2). \tag{55}$$

*Regions* 6 *and* 7. With use of (55), equations (37) to (43) yield

$$\begin{aligned}\varphi_7(t) &= c(t-\tau_5)+(\rho\varepsilon^*c)^{-1}[\gamma(\tau_5-\tau_4)-\lambda(\tau_5^2-\tau_4^2)/2+\tau_4(\alpha+\beta\tau_4/2)],\\ v_6(t) &= v_7(t) = [\gamma(t-\tau_4)-\lambda(t^2-\tau_4^2)/2+(\alpha+\beta\tau_4/2)\tau_4]/\rho\varphi_7(t),\\ \sigma_6(x,t) &= \sigma_7(x,t) = \sigma_y+\gamma-\lambda t-x[(\gamma-\lambda t)-\rho c v_7(t)]/\varphi_7(t),\\ \varepsilon_6 &= \varepsilon^*,\\ \varepsilon_7(x) &= (\rho c x)^{-1}\left\{\gamma\left[\tau_5+\frac{x-\varphi_5(\tau_5)}{c}-\tau_4\right]-\frac{\lambda}{2}\left[\left(\tau_5+\frac{x-\varphi_5(\tau_5)}{c}\right)^2-\tau_4^2\right]\right.\\ &\quad \left.+\tau_4(\alpha+\beta\tau_4/2)\right\}.\end{aligned} \tag{56}$$

The foregoing solutions are valid in the interval $\tau_5 \leq t < \tau_6 \leq \tau$. The value $\tau_6$ can be obtained from (56) by setting $\bar{\sigma}_{7'}(t) = \sigma_y$ and $t = \tau_6$, which yields

$$\tau_6 = \tau - \left(\frac{\sigma_y}{P_m}\right)(\tau - \tau_4) + \left[\left(\tau - \sigma_y \frac{(\tau - \tau_4)}{P_m}\right)^2 + \tau_4^2 + \tau_4(\tau - \tau_4)(P_m + P_0)/P_m - 2\tau_4\tau\right]^{1/2}. \tag{57}$$

From (57) we obtain the following conditions for $\tau_6 \leq \tau$:

$$\sigma_y < P_m < 2\sigma_y \quad \text{and} \quad \tau \geq (P_0\tau_4)/(2\sigma_y - P_m). \tag{58}$$

The condition that $\tau_6 > \tau$ is either

$$P_m \geq 2\sigma_y, \tag{59a}$$

or

$$\sigma_y < P_m < 2\sigma_y \quad \text{and} \quad \tau < (P_0\tau_4)/(2\sigma_y - P_m). \tag{59b}$$

As mentioned in section 2, the solution in $\tau \leq t < \tau_6$ in the latter case, which we denote by the subscripts 6′, 7′, is obtained from (41) to (43) by setting $p(t) = 0$ and replacing $G_5(t)$ by $G_5(\tau) - \sigma_y(t - \tau)$. This yields

$$\begin{aligned}
v_{6'}(t) &= v_{7'}(t) = \left[\gamma(\tau - \tau_4) - \frac{\lambda}{2}(\tau^2 - \tau_4) + (\alpha + \beta\tau_4/2)\tau_4 - \sigma_y(t - \tau)\right] \Big/ \rho\varphi_7(t), \\
\sigma_{6'}(x, t) &= \sigma_{7'}(x, t) = x[\sigma_y + \rho c v_{7'}(t)]/\varphi_7(t), \\
\varepsilon_{6'} &= \varepsilon^*, \\
\varepsilon_{7'} &= (\rho c x)^{-1}\left\{\gamma(\tau - \tau_4) - \frac{\lambda}{2}(\tau^2 - \tau_4) + (\alpha + \beta\tau_4/2) - \sigma_y\left[\frac{x - \varphi_5(\tau_5)}{c} + \tau_5 - \tau\right]\right\}, \\
&\quad \text{for } \varphi_7(\tau) \leq x < \varphi_7(\tau_6), \\
\varepsilon_{7'} &= \varepsilon_7(x) \quad \text{for } \varphi_7(\tau_5) \leq x \leq \varphi_7(\tau) \qquad \text{(cf. (56))}.
\end{aligned} \tag{60}$$

The solution in $\tau_5 \leq t \leq \tau$ (regions 6, 7) is again given by (56).

*Regions* 8–10. From (44)–(46), we have

$$\begin{aligned}
v_8 &= v_9 = v_{10} = 0, \\
\sigma_8 &= \sigma_9 = \sigma_{10} = \sigma_y + \gamma - \lambda t \quad \text{for } \tau_6 < t \leq \tau, \\
&\qquad = 0 \qquad\qquad\quad \text{for } t \geq \tau, \\
\varepsilon_8 &= \varepsilon^*, \qquad \varepsilon_9 = \varepsilon_7(x), \qquad \varepsilon_{10} = 0,
\end{aligned} \tag{61}$$

which corresponds to the first case (58).

*Example* 2.

Let us now assume that the slope of the segment AD in Fig. 1 is zero. In addition, let $P_0 = \sigma_y$ in (50). We have, therefore, the case of $p(t)$ increasing monotonically from zero to a maximum, and then decreasing monotonically to zero again. The solutions for this situation can be easily obtained from the Example 1 solutions in the limit as $c \to 0$ and $P_0 \to \sigma_y$.

## 4. CONCLUDING REMARKS

One-dimensional wave propagation in a semi-infinite, rigid, workhardening, locking rod, subjected to positive end pressure, was considered in this paper. It was demonstrated that closed-form solutions can be obtained in the entire $x$–$t$ plane provided (i) the constitutive relations of the rod are as indicated in Fig. 1, and either (ii) the initial loading is suddenly applied such that $p(0^+) \geq \sigma^*$, or (iii) the slope of the segment $EF$ in Fig. 1 is zero. In general, closed-form solutions (under (i)) can be obtained in all but region 3.†

## REFERENCES

[1] S. KALISKI, W. NOWACKI and E. WŁODARCZYK, On a certain closed solution for the shock-wave with rigid unloading. *Bull. Acad. pol. Sci. Sér. Sci. Techn.* **15,** 315–319 (1967).

[2] M. S. SAVADORI, R. SKALAK and P. WEIDLINGER, Waves and shocks in locking and dissipative media. *Proc. Am. Soc. civ. Engrs* **86,** 77–105 (1960).

[3] S. HANAGUD, Snow as a locking material–high pressure properties of snow. *Proc. Int. Conf. Low temperature Sci.*, Vol. 2, edited by H. ÔURA, pp. 807–826. Sapporo (1967).

(*Received* 19 *July* 1968; *revised* 24 *February* 1969)

**Абстракт**—Рассматривается одномерное распространение волны в полубесконечном, закрепленном стержне с упрочнением. Обсуждается общая задача. Получаются решения в замкнутом виде для отдельных специальных случаев. Ожидается, что это последнее даст возможность получить полезные системы для контроля численных программ, уставленных с целью сравнения с распространением волны в средах с комплексными определяющими законами. Обусловленное механическое поведение является также интересным, в своей сущности, ввиду того, что оказывается, качественно, типическим для грунтов в одноосном деформированном состоянии сжатия.

† Reference [2], which also deals with wave propagation in a locking medium came to the authors' attention after the completion of the present work. The two analyses differ in the following respects: Reference [2] deals with an elastic–perfectly plastic-locking medium under suddenly applied and then monotonically decreasing loads and the numerical results presented therein concentrate on behavior at the shock front, whereas the present work concerns a rigid–linearly workhardening-locking medium under suddenly applied and then decreasing or increasing loads and provides full field information. Uniaxial wave propagation in a multistage locking material has been discussed by Hanagud [3]. The material considered here may be approximately represented by a multistage locking material.